

RESEARCH ARTICLE

Neuronal upregulation of Prospero protein is driven by alternative mRNA polyadenylation and Syncrip-mediated mRNA stabilisation

Tamsin J. Samuels¹, Yoav Arava^{1,2}, Aino I. Järvelin¹, Francesca Robertson¹, Jeffrey Y. Lee¹, Lu Yang¹, Ching-Po Yang³, Tzumin Lee³, David Ish-Horowicz^{1,4} and Ilan Davis^{1,*}

ABSTRACT

During *Drosophila* and vertebrate brain development, the conserved transcription factor Prospero/Prox1 is an important regulator of the transition between proliferation and differentiation. Prospero level is low in neural stem cells and their immediate progeny, but is upregulated in larval neurons and it is unknown how this process is controlled. Here, we use single molecule fluorescent *in situ* hybridisation to show that larval neurons selectively transcribe a long *prospero* mRNA isoform containing a 15 kb 3' untranslated region, which is bound in the brain by the conserved RNA-binding protein Syncrip/hnRNPQ. Syncrip binding increases the stability of the long *prospero* mRNA isoform, which allows an upregulation of Prospero protein production. Adult flies selectively lacking the long *prospero* isoform show abnormal behaviour that could result from impaired locomotor or neurological activity. Our findings highlight a regulatory strategy involving alternative polyadenylation followed by differential post-transcriptional regulation.

This article has an associated First Person interview with the first author of the paper.

KEY WORDS: Prospero, Syncrip, mRNA stability, Neuroblast, Post-transcriptional regulation

INTRODUCTION

The central nervous system (CNS) consists of a huge diversity and number of neurons that originate from a limited population of neural stem cells (NSCs) (Kelava and Lancaster, 2016), also known as neuroblasts (NBs) in *Drosophila*. To produce a normal CNS, NBs must divide the correct number of times and their progeny must undergo a precisely regulated programme of differentiation. Many factors and mechanisms regulating these processes have been studied in detail, and are extensively conserved between vertebrates and *Drosophila* (Homem and Knoblich, 2012). The emphasis in the field has been on identifying key transcription factors and their downstream transcriptional effects. However, post-transcriptional

regulation, which can modulate protein expression with enhanced spatial and temporal precision, has been less well characterised.

In *Drosophila* embryos and larvae, NBs undergo repeated asymmetric divisions, maintaining a single large cell that retains its stem cell properties. Each division of a type I NB also produces a ganglion mother cell (GMCs), which divides only once to generate a pair of neurons (Homem and Knoblich, 2012; Knoblich, 2008). Type I NB lineage differentiation is regulated by the conserved homeodomain-containing transcription factor, Prospero (Pros)/Prox1 (Bayraktar et al., 2010). Pros activates the expression of genes required for the differentiation of type I NB progeny and suppresses the expression of genes that promote stem cell-like properties (Bello et al., 2006; Betschinger et al., 2006; Choksi et al., 2006; Doe et al., 1991; Lai and Doe, 2014; Lee et al., 2006; Matsuzaki et al., 1992; Vaessin et al., 1991). *pros* mRNA and Pros protein are expressed in the NBs, but are excluded from the nucleus and segregated asymmetrically into the GMC during NB division (Hirata et al., 1995; Kitajima et al., 2010; Knoblich et al., 1995; Spana and Doe, 1995). In this way, the sub-cellular localisation of Pros allows the stem cell-like properties of NBs to be maintained, while ensuring that their GMC progeny differentiate correctly. In embryonic type I NBs, Pros is expressed in GMCs and new-born neurons, but is quickly switched off as neurons mature (Srinivasan et al., 1992). In contrast, Pros expression is upregulated in larval neurons and is required to maintain neuronal identity (Carney et al., 2013), but the mechanism controlling this upregulation is not known.

Here, we examine the mechanism of upregulation of Pros expression in larval neurons using single molecule fluorescent *in situ* hybridisation (smFISH) and immunofluorescence (IF) in whole-mount brains (Yang et al., 2017b). We observe hugely increased *pros* mRNA expression in neurons, correlated with upregulated Pros protein. This highly expressed neuronal *pros* mRNA includes an unusually long 15 kb 3' untranslated region (UTR) (*pros^{long}*). *pros^{long}* is not produced in embryos or in larval NBs, but is switched on in larval neurons. We show that *pros^{long}* is stabilised by binding to the conserved RNA-Binding Protein (RBP), Syncrip (Syp)/hnRNPQ (Kuchler et al., 2014; Liu et al., 2015; McDermott et al., 2014, McDermott et al., 2012). We find that the *pros* 3' UTR extension is required for the neuronal upregulation of Pros protein. Our observations highlight a novel example of alternative polyadenylation followed by differential post-transcriptional regulation through mRNA stability, which controls the level of protein expression in distinct cell types.

RESULTS

Upregulation of Pros protein in neurons is achieved through cell type-specific stabilisation of *pros* mRNA

Pros protein is expressed at low levels in larval type I NBs and GMCs, where it promotes GMC differentiation, and is then upregulated in larval neurons (Carney et al., 2013; Choksi et al., 2006). To determine

¹Department of Biochemistry, The University of Oxford, Oxford, OX1 3QU, UK.

²Department of Biology Technion, Haifa, 32000, Israel. ³Howard Hughes Medical Institute, Janelia Research Campus, 19700 Helix Drive, Ashburn, VA, 20147 USA.

⁴MRC Laboratory for Molecular Cell Biology, University College, London, WC1E 6BT UK.

*Author for correspondence (ilan.davis@bioch.ox.ac.uk)

ORCID: T.J.S., 0000-0003-4670-1139; A.I.J., 0000-0002-1225-4396; F.R., 0000-0002-1737-1073; J.Y.L., 0000-0002-5146-0037; T.L., 0000-0003-0569-0111; D.I., 0000-0001-5684-7129; I.D., 0000-0002-5385-3053

This is an Open Access article distributed under the terms of the Creative Commons Attribution License (<https://creativecommons.org/licenses/by/4.0>), which permits unrestricted use, distribution and reproduction in any medium provided that the original work is properly attributed.

whether the upregulated Pros expression in neurons is driven by an increase in *pros* mRNA levels or by increased Pros translation, we used smFISH in whole-mount *Drosophila* larval brains at the wandering third instar stage (Yang et al., 2017b). We carried out four-colour imaging with smFISH against *pros* exon (Fig. 1A), anti-Pros antibody (marking differentiated neurons) and DAPI (marking DNA in all cells) (Fig. 1B). NBs were easily identified by their large cell size. As previously shown (Carney et al., 2013; Choksi et al., 2006), we found that Pros expression is low in NBs and GMCs (outlined in white and pink, respectively) and is upregulated in Elav⁺, post-mitotic neurons (Fig. 1B). *pros* exon smFISH signal is also upregulated in Elav⁺ cells, and correlates with the increased Pros protein expression (Fig. 1B). We conclude that increased *pros* transcript number is responsible for the increased Pros protein expression in the neurons compared to NBs.

We then asked whether the increase in *pros* mRNA level in neurons is regulated at the level of transcription, or post-transcriptionally through mRNA stability. We used smFISH with *pros* intron-specific probes to visualise the *pros* transcription foci (Fig. 1A,C). There are two transcription foci in each cell (these are paired in the progeny cells, thus visible as a single combined focus

of higher intensity). Unexpectedly, we observed bright transcription foci in the type I NBs, but very few cytoplasmic transcripts in these cells (Fig. 1C, white outline). This result suggests that *pros* mRNA is more unstable in NBs than in neurons, where much higher levels of *pros* mRNA accumulate.

pros mRNA in larval brains contains an exceptionally long 3' UTR

Post-transcriptional regulation is often linked to expression of distinct alternative mRNA isoforms, and neurons have been shown to selectively express transcript isoforms with unusually long 3' UTRs (Hilgers et al., 2012, 2011; Oktaba et al., 2015). Therefore, we examined the *pros* isoform usage in the type I NB lineage.

pros is annotated in FlyBase as having six isoforms with three different 3' UTR lengths: ~1 kb, ~3 kb and ~15 kb (Fig. 2A, FB2019_05, Thurmond et al., 2019). To test which isoforms are expressed in larval brains, we carried out northern blots. Our northern blot analysis used a probe that is common to all the annotated isoforms of *pros* transcripts (probe ALL) and detected the known ~6 kb isoform in embryos (Fig. 2A,B) (Doe et al., 1991; Matsuzaki et al., 1992; Vaessin et al., 1991). In larval brain extracts, the northern

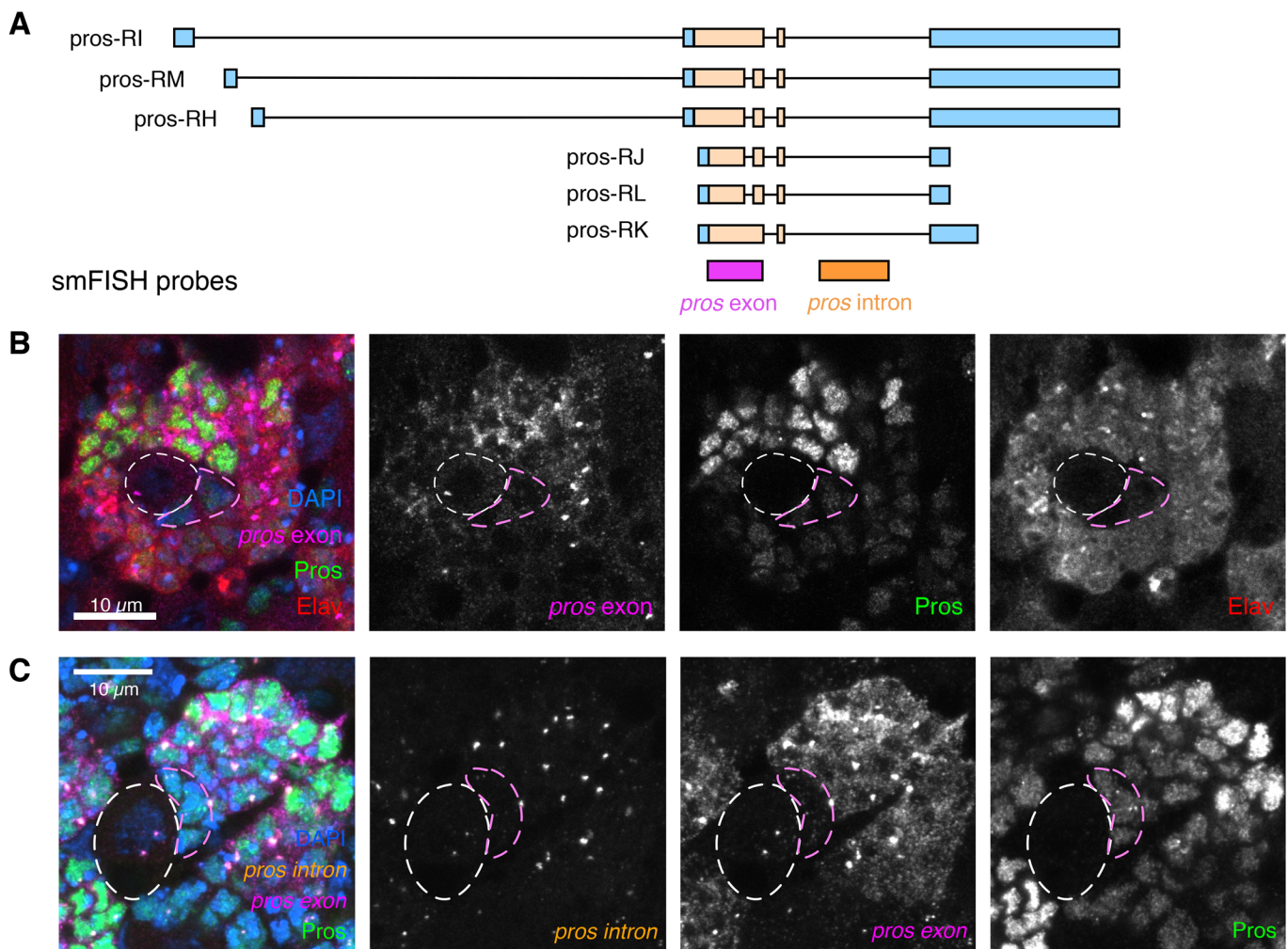


Fig. 1. *Pros* cell type-specific expression is regulated post-transcriptionally. (A) Illustration of smFISH probe positions on the *pros* mRNA transcript isoforms. (B) Third instar larval brains stained for smFISH against *pros* exon, with IF against Elav and Pros. *pros* mRNA is upregulated in post-mitotic neurons (marked with Elav), and this correlates with upregulated Pros protein. (C) smFISH against the *pros* intron and *pros* exon (probe positions shown in A) together with IF against Pros protein, shows that *pros* is transcribed in all cells of the Type I NB lineage, even in NBs where there are low levels of Pros protein and *pros* mRNA. Scale bars: 10 μm. NB, white dashed outline; GMC, pink outline.

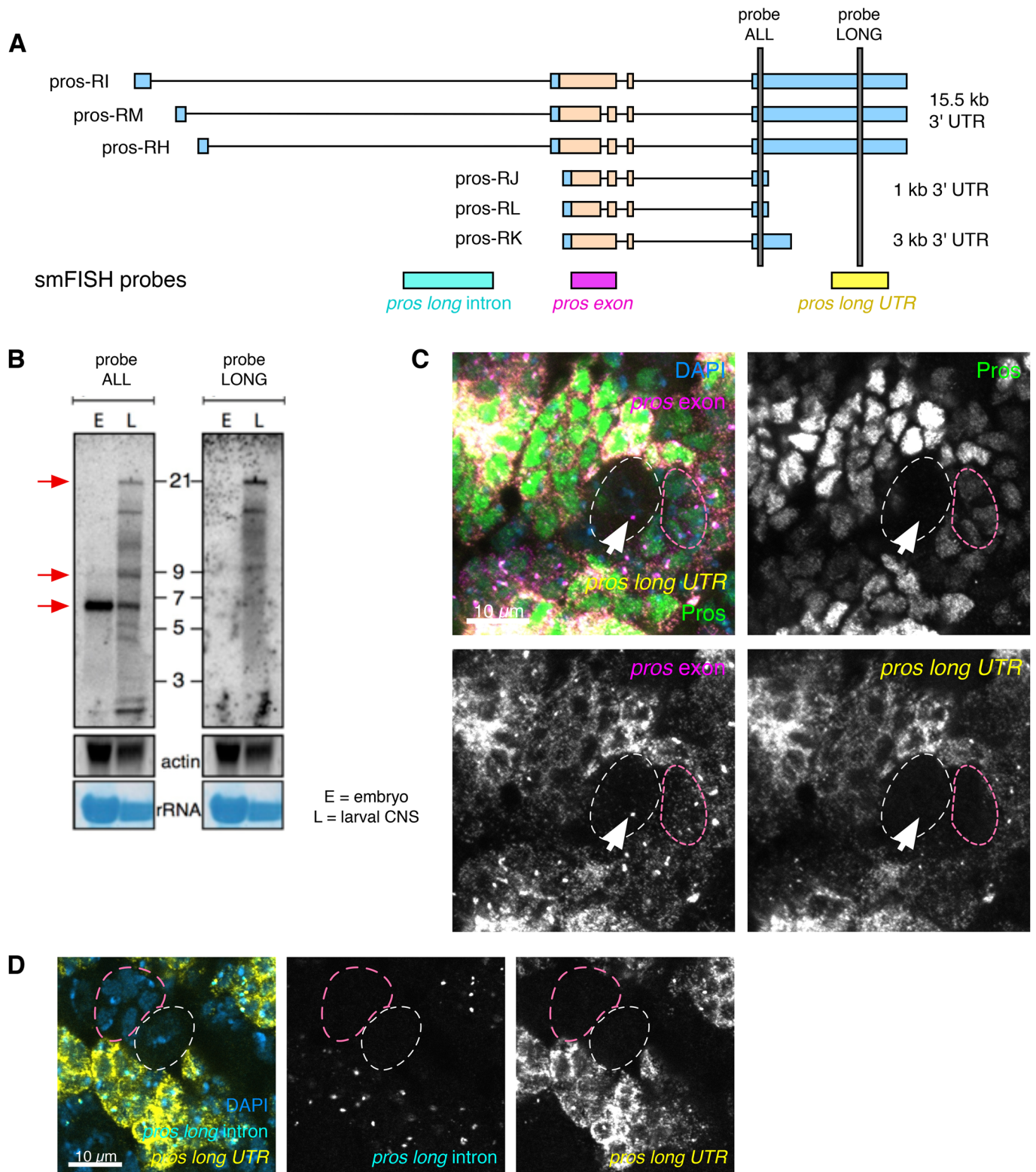


Fig. 2. *pros^{long}* isoform is expressed in larval brains and is specifically transcribed in larval neurons. (A) Diagram showing annotated *pros* transcript isoforms and the position of smFISH (*pros long intron*, *pros* and *pros long UTR*) and northern blot probes (grey bars). (B) Northern blot confirms the existence of multiple *pros* mRNA isoforms at 6 kb, 9 kb and 21 kb (red arrows) in the larval CNS. The 21 kb isoform corresponds to *pros* transcript with 15 kb 3' UTR. E, embryo; L, larval CNS. (C) Costaining with *pros* exon and *pros long UTR* smFISH and Pros IF shows that *pros^{long}* RNA is detected only in neurons. In the NB (white dotted outline), or the GMCs (pink dotted outline), *pros* exon is detected without *pros long UTR*. Pros protein is upregulated in cells expressing *pros^{long}*. (D) *pros long intron* probe only recognises the nascent transcripts of the *pros^{long}* isoform. *pros long intron* is detected exclusively in neurons, and not in the NB (white dotted outline) or GMCs (pink dotted outline). Scale bars: 10 μ m.

blots show multiple-sized *pros* transcripts including isoforms approximately 6 kb, 9 kb and 21 kb in length (Fig. 2B), corresponding to 3' UTR lengths of 1 kb, 3 kb and 15 kb, respectively. We also detected the 21 kb *pros* band in larval brains using a probe targeting the extended region of the 15 kb 3' UTR (Fig. 2A,B). We conclude that embryos express only the shortest isoform of *pros*, whereas larval brains express two additional isoforms, with 3 kb and 15 kb long 3' UTRs, respectively.

To investigate the cell type-specific expression of the *pros* isoforms in larval brains, we performed smFISH experiments using a probe specific to the shared coding exon (*pros*) and a probe that is specific to the extended region of the 15 kb 3' UTR region (*pros long UTR*) of the *pros^{long}* transcripts (defined as the isoforms containing the 15 kb 3' UTR), co-stained for Pros protein (Fig. 2A, C). *pros^{long}* is highly expressed in the cells with highest *pros* exon signal, and correlates well with upregulated Pros protein. We conclude that the upregulated *pros* mRNA in neurons consists primarily of *pros^{long}*. Co-staining with Elav to label neurons shows that *pros^{long}* is expressed specifically in neurons and is absent from NBs and GMCs (Fig. S1A). However, GMCs do show low levels of *pros* exon smFISH signal and Pros protein (Fig. 2C, outlined in dashed pink). These observations suggest that the short isoform of *pros* produces the low levels of Pros seen in the GMCs and NBs.

To determine precisely where *pros^{long}* is transcribed in the brain, we visualised *pros^{long}* transcription using smFISH with intron probes specific for the long isoforms (Fig. 2A,D). We detected *pros^{long}*-specific transcription foci only in neurons, where we also observed *pros long UTR* smFISH signal in the cytoplasm. In contrast, no *pros^{long}* intron signal was detected in the NBs or GMCs (Fig. 2D outlined in dashed white and pink, respectively). We conclude that the *pros^{long}* isoform is specifically transcribed in larval neurons. Our results support a model in which a low level of Pros protein is produced by the short *pros* isoform in NBs and GMCs. Transcription of *pros^{long}* is switched on in the larval neurons and this isoform is stabilised, resulting in higher *pros* mRNA levels and upregulated Pros protein.

Syp is expressed in the type I NB lineage and stabilises *pros* mRNA

Post-transcriptional regulation, including mRNA stability, depends on the binding and action of specific RBPs. We have previously shown in larval extracts that *pros* mRNA associates with Syp, a highly conserved RBP (McDermott et al., 2014). Syp is a key factor in the temporal regulation of larval NBs and is known to regulate the transcription factor Chinmo to determine neuron fate (Liu et al., 2015; Ren et al., 2017; Syed et al., 2017). Syp is expressed in the larval type I NBs and their progeny (Fig. 3A) (Liu et al., 2015), and so we tested whether Syp binds *pros* mRNA in the larval brain. 58.3% of *pros* mRNA was co-immunoprecipitated with Syp in larval brain lysates, while only 3.2% of *rp49*, a control RNA, was pulled down (Fig. 3B,C). These results demonstrate that Syp binds specifically to *pros* RNA, rendering Syp a good candidate for an upstream regulator of *pros* mRNA stability.

To determine whether Syp regulates the levels of *pros* mRNA, we compared levels of *pros* transcription, cytoplasmic *pros* transcripts and Pros protein in brains mutant for a *syp* allele that lacks Syp protein (see Materials and Methods). The results show that Pros protein is reduced in the neurons of *syp* mutant brains (Fig. 3D). Pros protein levels are maintained at low levels in the *syp* mutant neurons but the upregulation of Pros is lost. *pros* mRNA is also very substantially reduced in the *syp* mutants, most obviously in the neurons (Fig. 3D). We measured the intensity of *pros* intron signal at

the transcription foci in *wild type* and *syp* mutant brains (Fig. 3E) and observed a small but significant increase in *pros* transcription in the *syp* mutant type I NBs, compared to *wild type* (1.3-fold increase). In progeny cells (pooled neurons and GMCs) there is no significant change in *pros* transcription in the *syp* mutant, compared to the *wild type* (Fig. 3E). Therefore, changes in *pros* transcription are not responsible for the reduction of *pros* transcripts in the *syp* mutant. We suggest that Syp mediates the upregulation of Pros protein in neurons primarily by stabilising cytoplasmic *pros* mRNA.

Syp negatively regulates the RBP Imp/IGF2BP in type I NBs (Liu et al., 2015) and therefore could regulate *pros* mRNA stability indirectly via Imp. To distinguish whether Syp regulates *pros* directly or indirectly, we compared the levels of *pros* mRNA and Pros protein in *syp* knockdown and *imp syp* double-knockdown brains (Yang et al., 2017a) (Fig. S1B). *imp syp* double-knockdown phenocopies the single *syp* knockdown (Fig. S1B). Combined with the *pros* pull-down in Syp immunoprecipitations, these results indicate that Syp's effects on *pros* are independent of its effects on Imp.

pros^{long} is stabilised by Syp

Loss of Syp has the greatest effect on *pros* in the neurons. In *syp* mutant neurons *pros* mRNA is substantially reduced and Pros protein upregulation is lost. We have previously shown that *pros^{long}* is responsible for the neuronal *pros* mRNA and protein upregulation, so we asked whether Syp acts specifically on *pros^{long}*. We used smFISH against the *pros^{long}* 3' UTR in *syp* mutant larval brains and found that it is substantially reduced in neurons, compared to *wild type* (Fig. 4A). We co-stained with the *pros^{long}*-specific intron probe and found that *pros^{long}* is transcribed normally in the *syp* mutant. We conclude that Syp upregulates Pros protein in neurons by stabilising *pros^{long}* mRNA.

To confirm that the loss of cytoplasmic *pros* mRNA in *syp* mutants is due to specific loss of the long isoform, we carried out transcriptomic analysis of *syp* mutant versus *wild type* brains (Table S1). The results show that the abundance of *pros^{long}* is specifically reduced in *syp* mutant brains, whereas the shorter *pros* forms are maintained (Fig. 4B,C). Northern blot analysis confirmed these findings (Fig. 4D).

pros^{short} is sufficient to maintain neuronal fate

We have shown that Syp is required for the upregulation of Pros protein in larval neurons, and this occurs through the regulated mRNA stability of *pros^{long}*. When Pros is depleted from neurons, but not NBs or GMCs, such as in the *midlife crisis* mutant, this leads to loss of neuronal differentiation and expression of NB genes (Carney et al., 2013). Therefore, we used the *syp* mutant as a tool to examine the specific role of the upregulated Pros protein levels in neurons, as opposed to the effect of loss of all Pros protein from the neurons. Unexpectedly, we found that neuronal differentiation progresses normally in *syp* mutants and neurons do not revert to NBs, as they do not switch on the NB marker, Dpn. We used clonal analysis to mark individual NB lineages in *wild type* and *syp* mutant brains and stained with Dpn, Pros and Elav (Fig. 5). Each *syp* mutant clone contained just one Dpn positive NB, and Elav was expressed in the progeny cells, demonstrating their neuronal identity. We conclude that the stabilisation of *pros^{long}* by Syp in progeny cells is not required for the normal neuronal path of differentiation nor to prevent reversion of neurons to NBs. The remaining low level of Pros in the neurons of the *syp* mutant, provided by the short *pros* mRNA isoform, is sufficient to prevent reversion to an NB fate.

The question remains: what is the function of *pros^{long}* mRNA? A burst of nuclear Pros protein is known to have an important role in

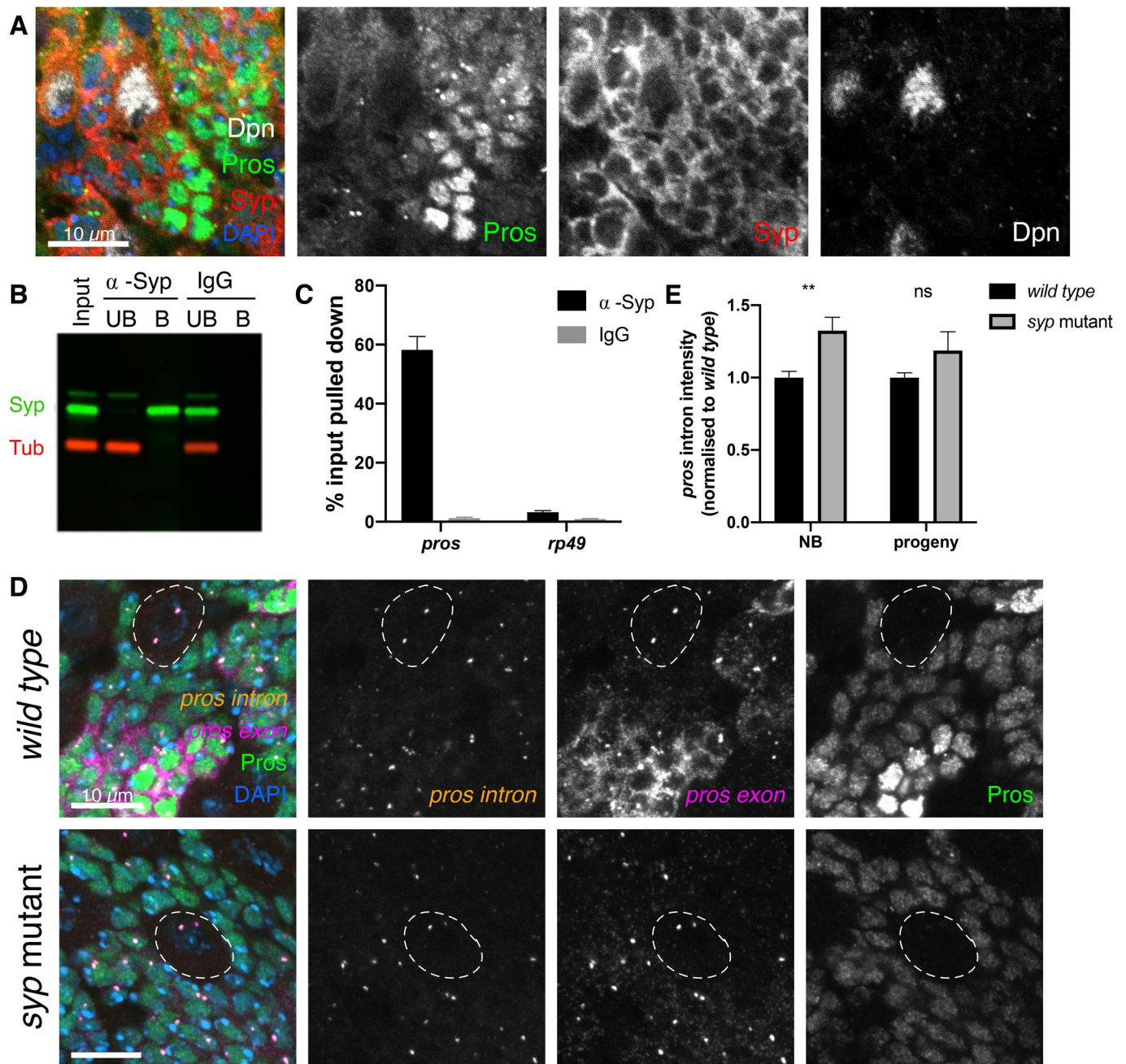


Fig. 3. Syncrip selectively stabilises the *pros*^{long} isoforms in neurons. (A) Syncrip (Syp) protein is expressed in the type I NB (marked with Dpn) and progeny lineage in third instar larvae. Syp is also expressed in the neurons, where Pros is upregulated. (B) Western blot confirms Syp is immunoprecipitated (IP) selectively and efficiently. α -Tubulin (Tub) was used as negative control. (C) *pros* mRNA is enriched by Syp IP (58.3% of input pulled down) but not by IgG control IP (1.3%). Negative control, ribosomal *rp49* (α -Syp: 3.2%, IgG: 0.9%) ($n=7$). Error bars represent s.e.m. (D) Loss of Syp has a minimal effect on transcription levels indicated by *pros* intron, but *pros* exon signal and Pros protein are greatly reduced. NBs outlined in white. (E) Intensity of *pros* intron signal in *wild type* and *syp* mutant. Normalised to *wild type* for each experiment. Significance was calculated using *t*-tests. ** $P<0.01$, ns=not significant $P>0.05$. NB, sum of intensity of two transcription foci; progeny, intensity of single spot including both transcription foci. Scale bars: 10 μ m.

terminating NB divisions in pupae (Kohwi and Doe, 2013; Maurange et al., 2008). Furthermore, Syp is required for the final symmetric division that terminates the type I NB in the pupa (Yang et al., 2017a). In the *wild type* pupal brain, all type I NBs, except the mushroom body NBs, terminate by 48 h after pupal formation (APF) (Siegrist et al., 2010). Syp-depleted type I NBs persist in the pupal brain for more than 48 h APF (Yang et al., 2017a). We surmised that *pros*^{long} might be required at the terminal division, stabilised by Syp to allow the upregulation of Pros in the NB. To test

this hypothesis we produced a series of transgenic lines aiming to remove *pros*^{long}.

Several attempts to generate flies selectively deleting the *pros*^{long} transcripts were unsuccessful. These included a frame shift mutation, which did not introduce nonsense-mediated mRNA decay (NMD) of the long *pros* isoforms (Fig. S2; Materials and Methods), and attempting a direct deletion of the *pros* 3' UTR extension (Materials and Methods). We successfully deleted the three promoters that are annotated to produce *pros*^{long} (Fig. S3A), but found that the 3' UTR

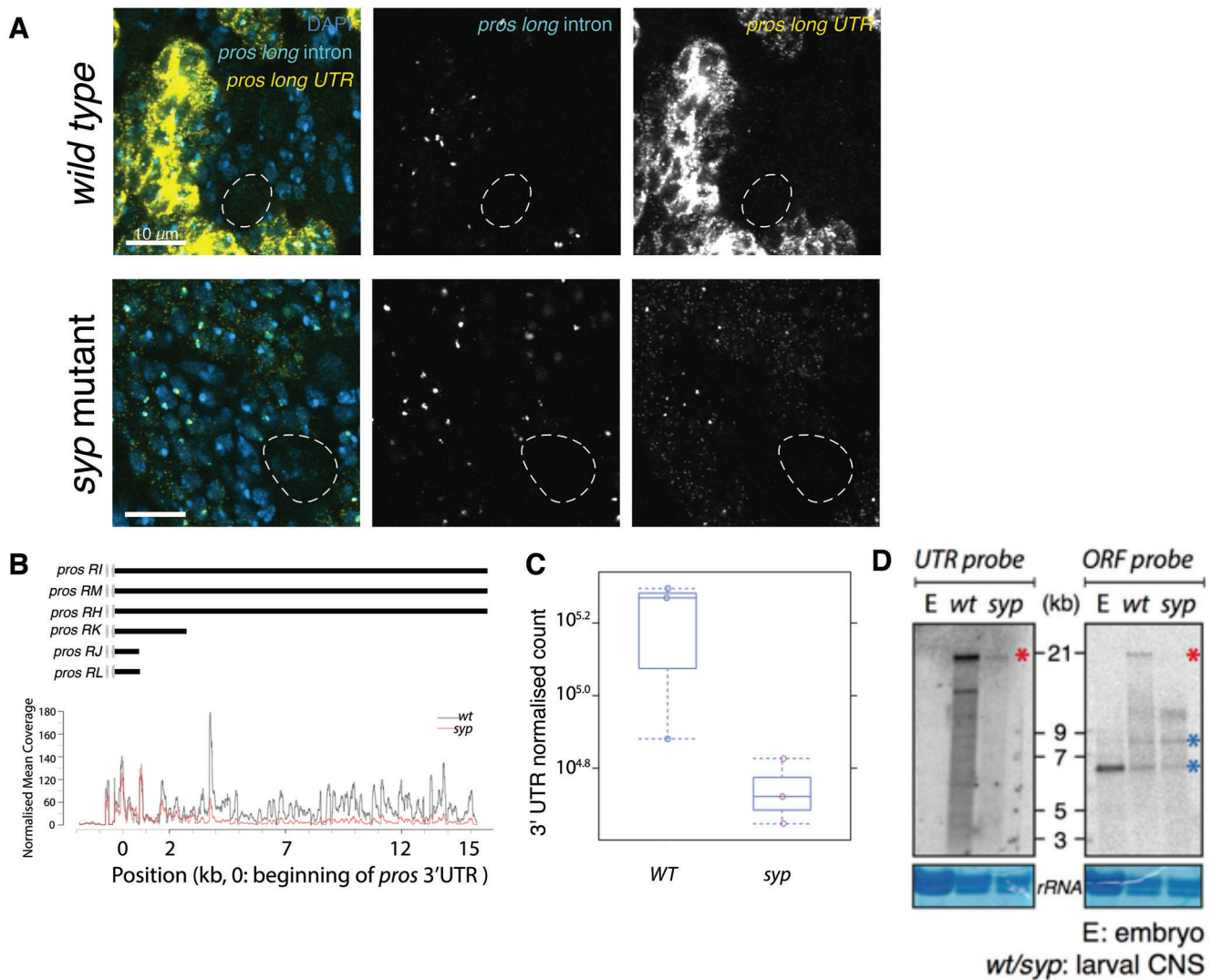


Fig. 4. Syncrip selectively stabilises the *pros*^{long} isoforms in neurons. (A) smFISH against *pros* long intron and *pros* long UTR shows that *pros*^{long} is normally transcribed in the *syp* mutant. (B) RNA sequencing shows selective loss of *pros*^{long} isoform in *syp* mutants. Read coverage for the first 3 kb of *pros* 3' UTR is not different between *wild type* (wt) and *syp* mutant whereas the distal 12 kb of *pros* 3' UTR is reduced in *syp* mutants. (C) Quantitative analysis of total sequencing reads of *pros* 3' UTR in *wild type* and *syp* mutants. (D) Northern blot showing the selective loss of *pros*^{long} isoforms in *syp* mutants. The intensity of the 6.5 kb and 9 kb bands are similar between *wild type* and *syp* mutants (blue asterisks) whereas the 21 kb band is reduced in *syp* mutants (red asterisk). Scale bars: 10 μ m.

extension of *pros*^{long} can be transcribed from the downstream promoters (Fig. S3B) and there was no change in Pros protein expression (Fig. S3C). Finally, we used a strong SV40 transcriptional terminator to terminate transcription at the beginning of the 3' UTR extension (see Materials and Methods). The SV40 terminator reduced but did not entirely remove the extended UTR of *pros*^{long} (Fig. S4).

Unexpectedly, the inserted *dsRED* marker used to screen for integration (*proslong-REDr*; Materials and Methods) does terminate the 3' UTR extension of *pros* (Fig. 6), allowing us to test the effect of removing the 3' UTR extension.

smFISH against the *pros* exon and *pros*^{long} 3' UTR showed that the long 3' UTR is almost entirely lost in the *proslong-REDr* brains (Fig. 6). Therefore, regulation of *pros* mRNA through the 3' UTR extension is disrupted in this line. The signal from the *pros* exon probes is reduced compared to the *wild type*, but remains higher than in the *syp* mutant, which could be explained by residual binding of

Syp to *pros*^{long} in regions outside the UTR extension. Alternatively, Syp may stabilise multiple isoforms of *pros*.

In order to understand the role of *pros*^{long} in regulating Pros protein expression, we examined Pros protein level in *proslong-REDr* brains. We found that the cell type-specific upregulation of Pros protein in neurons is lost in *proslong-REDr* brains (Fig. 7A), which is consistent with the 3' UTR extension of *pros* being required for the neuronal upregulation of Pros protein during larval neurogenesis.

To test the function of *pros*^{long} in NB termination, we examined the number of NBs remaining at 48 h APF. We found that *pros*^{long} is not required for normal NB termination. At 48 h APF, *wild type* pupae have only four NBs remaining [labelled with Dpn, the mushroom body (MB) NBs], while *syp* mutant pupal brains contain many persistent NBs (Fig. 7B). In the *proslong-REDr* brains, we observe only the four MB NBs at 48 h APF, showing that the type I NBs terminate normally, despite the loss of the *pros*^{long} 3' UTR extension.

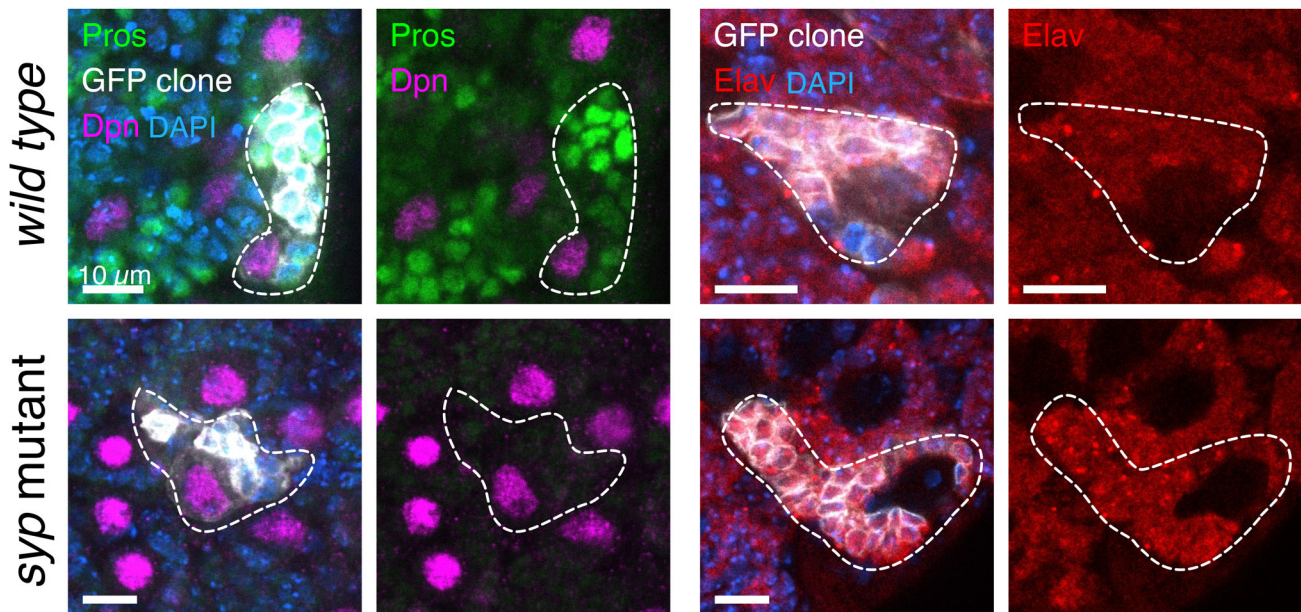


Fig. 5. *Syp* and *pros^{long}* are not required to maintain larval neurons in differentiated states. Clonal analysis shows normal GMC differentiation in the *syp* mutant. Type I NB lineage clones are marked with *mCD8::GFP* (outlined with white trace) and stained with IF against *Pros*, *Dpn* (*wild type* $n=7$, *syp* $n=9$) and *Elav* (*wild type* $n=16$, *syp* $n=4$). Both *wild type* and *syp* mutant clones have a single *Dpn*-expressing cell per clone and the progeny cells express *Elav*, marking a neuronal fate.

We tested whether *pros^{long}* is required for neuronal fate specification. *Syp* controls α/β neuronal fate during MB development, and loss of *Syp* results in complete loss of α/β neurons and precocious production of γ neurons (Liu et al., 2015). Single-cell transcriptomic analysis of the adult *Drosophila* brain has revealed that α/β neurons express much higher levels of *pros* compared to γ and α'/β' neurons (Davie et al., 2018). To test whether stabilisation of *pros^{long}* by *Syp* is required for the specification of α/β neurons, we examined the MB morphology in 1-day old *proslong-REDr* adult brains (Fig. 7C). Immunostaining against FasII showed the overall morphology of α/β and γ neurons in the *proslong-REDr* brains are comparable to the *wild type* control, indicating that fate patterning of MB neurons occurs normally even in the absence of *pros^{long}*.

Finally, we wondered whether *pros^{long}* is required in adult flies. We found that adult flies lacking *pros^{long}* show highly penetrant behavioural defects. The majority of *proslong-REDr* adult flies eclose normally and are morphologically normal, but display an abnormal behaviour consistent with impaired locomotor or neurological activity (Movie 1). The same phenotype is also seen in hemizygous *proslong-REDr* flies (Movie 2), implying that it indeed derives from depletion of the *long* mRNA isoform. This phenotype indicates that the *pros^{long}* mRNA isoform has a function in the adult brain, although its detailed characterisation is beyond the scope of this study.

DISCUSSION

Many key regulators of NB proliferation and differentiation have been identified and characterised (Grosskortenhaus et al., 2006; Isshiki et al., 2001; Kambadur et al., 1998; Kohwi and Doe, 2013; Li et al., 2013; Narbonne-Reveau et al., 2016; Novotny et al., 2002; Pearson and Doe, 2003). Recently, an increasing number of RBPs, the key regulators of post-transcriptional processes, have been implicated in neurodevelopment (Betschinger et al., 2006; Hilgers et al., 2012; Liu et al., 2015), suggesting that the importance of post-transcriptional regulation in the brain has so far been

underestimated. Here, we have applied smFISH to examine the regulation of the transcription factor (TF) *Pros*, a master switch promoting neuronal differentiation. We show that *Pros* expression is regulated by the differential stability of its mRNA isoforms depending on their 3' UTR lengths. Unstable *short* mRNA isoforms produce sufficient *Pros* protein to prevent GMCs and their neuronal progeny from reverting back to NB identity, but a switch to the more stable *pros^{long}* isoforms is required to upregulate *Pros* protein in larval neurons. Our findings highlight the capacity of cell type-specific alternative 3' UTRs to mediate different modes of post-transcriptional regulation of mRNA isoforms.

Low-level *pros^{short}* has a distinct function from high-level *pros^{long}*

Surprisingly, we found that neurons do not de-differentiate into NBs in *syp* mutants, despite the loss of neuronal *Pros* upregulation in the absence of *pros^{long}*. Previous work has shown that *Pros* elimination in young or middle-aged larval neurons causes de-differentiation of neurons and their reversion to NBs (Bello et al., 2006; Betschinger et al., 2006; Carney et al., 2013; Lee et al., 2006). Our work suggests that the low levels of *Pros* remaining in the *syp* mutant (provided by *pros^{short}*) are sufficient for neurons to maintain their identity. *pros^{long}* is not required to drive differentiation of GMCs to neurons or to maintain neuronal identity. Although we have not uncovered the function of *pros^{long}* in larval/pupal brain development, the impaired locomotive activity of the *proslong-REDr* adult flies indicates a role of *pros^{long}* in the adult brain, either because of an earlier neuronal specification event or due to a function of *Pros* in the adult brain.

The 15 kb *pros* UTR extension allows multiple levels of post-transcriptional regulation

Exclusion of the 3' UTR extension from *pros* transcripts in the *proslong-REDr* brains reduces the number of *pros* transcripts and *Pros* protein in the neurons. However, the *pros* transcript levels

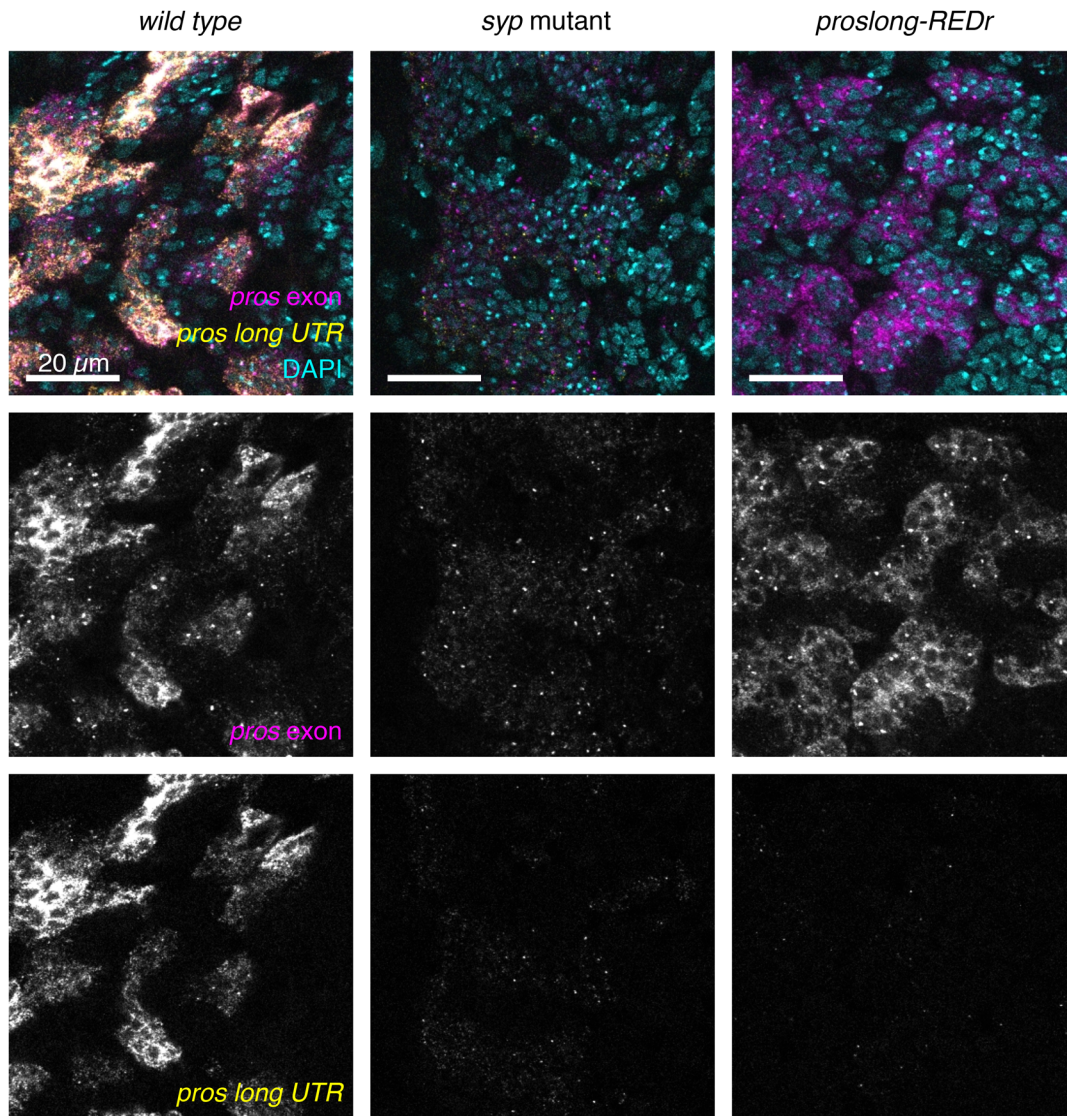


Fig. 6. *proslong-REDr* terminates transcription of the *pros* UTR extension. Insertion of a dsRED marker in reverse orientation downstream of the 3 kb UTR termination signal (*proslong-REDr*) results in loss of the *pros* UTR extension (visualised with the *pros long UTR* smFISH probe). The *pros exon* smFISH shows that *proslong-REDr* expresses higher levels of *pros* than *syp* mutant brains, but much less than *wild type*. Scale bars: 20 μ m.

are still much higher in *proslong-REDr* than in *syp* mutant brains. This residual *pros* signal suggests that Syp can stabilise *pros* mRNA through binding to additional regions of the transcript, perhaps the 5' UTR sequence that is also unique to the *pros^{long}* transcripts, or some shared sequence included in all transcripts.

The 3' UTR extension of *pros^{long}* may mediate a second regulatory step, at the level of translation. The upregulation of Pros protein in the neurons is lost in the *proslong-REDr* brains, despite the relatively high levels of remaining *pros* mRNA transcripts. While the *pros exon* smFISH signal is much higher in the *proslong-REDr* brains, compared to the *syp* mutant, the Pros protein levels are similar between the two genotypes. This result suggests that the *pros^{long}* 3' UTR extension includes additional regulatory sequences that promote increased *pros* translation, either via Syp or an unidentified second RBP. This hypothesis would explain why a moderate decrease in *pros* transcript levels in *proslong-REDr* brains leads to a loss of neural Pros protein upregulation.

Post-transcriptional and transcriptional regulation work hand-in-hand to achieve cell-type-specific gene expression

Our experiments show that Pros expression is controlled at two levels: alternative polyadenylation and then differential mRNA stability, regulated through Syp binding. The molecular mechanism underlying the cell type-specific choice of *pros* isoform has not yet been identified. In *Drosophila* embryos, Elav is recruited at the promoter of extended genes and is required to extend the 3' UTR of *brat* (Hilgers, 2015; Oktaba et al., 2015). Future experiments will determine whether *pros* differential polyadenylation is regulated at the promoter region by a similar Elav-dependent mechanism.

Many key regulators in the brain also have complex gene structures such as multiple isoforms and long 3' UTRs, hallmarks of post-transcriptional mechanisms (Berger et al., 2012; Hilgers et al., 2011; Stoiber et al., 2015; Tekotte et al., 2002). Such genes include the temporal regulator neuronal fate, *chinmo* (Liu et al., 2015), the driver of cell growth and division, *myc* (Samuels et al., 2020) and the mRNA-binding proteins, *brat* (Bello et al., 2006; Betschinger et al., 2006; Lee et al., 2006) and *imp* (Liu et al., 2015). Quantitative

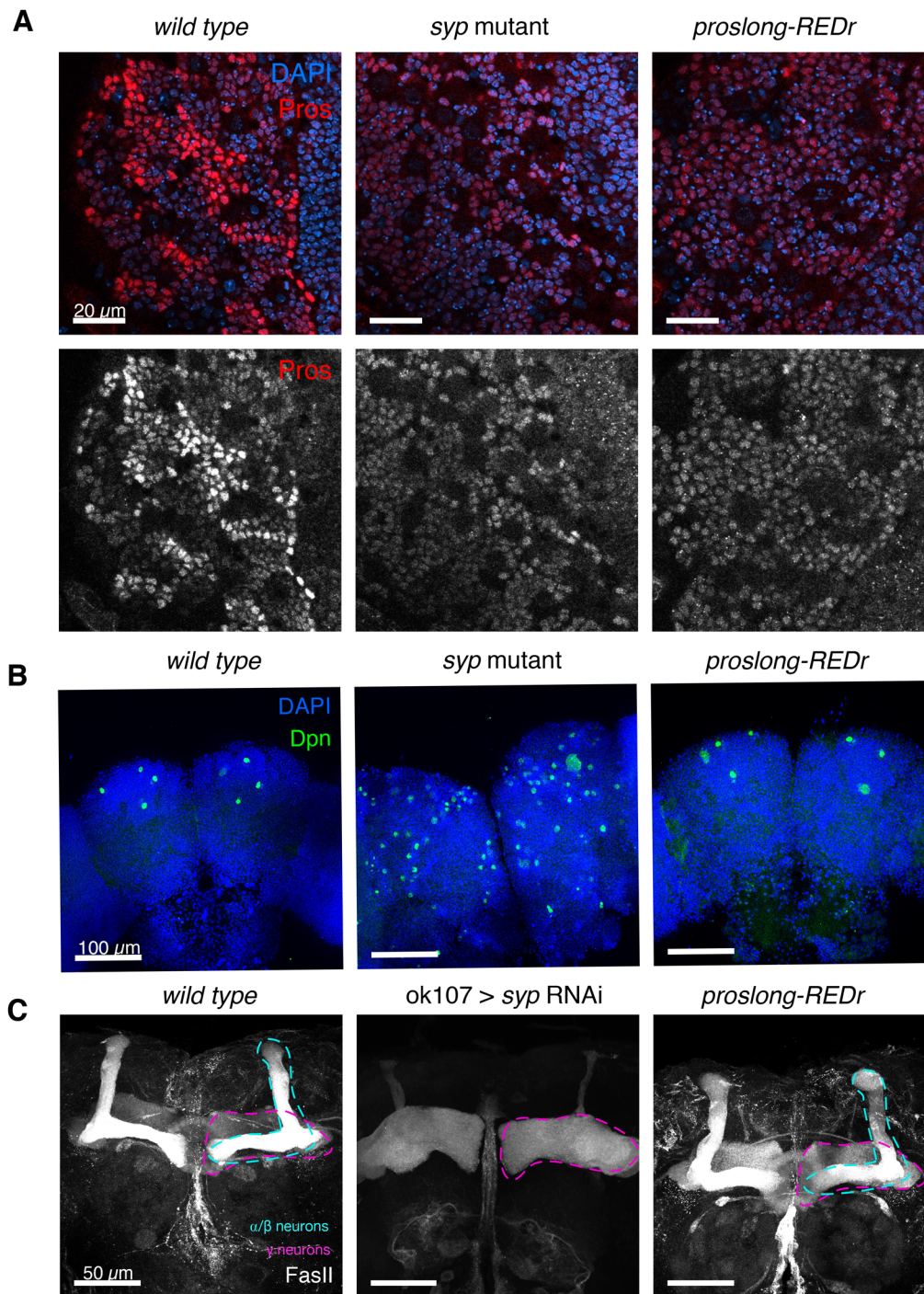


Fig. 7. Loss of *pros*^{long} blocks Pros protein upregulation but has no effect on NB termination. (A) Pros protein level is not upregulated in the neurons of *proslong-REDr* larval brains. (B) Dpn marks NBs in pupal brains, 48 h APF. In *wild type*, only the four MB NBs remain. In the *syp* mutant, many NBs are long-lived in the pupal brain. In the *proslong-REDr* brains, type I NBs terminate normally and only the four MB NBs persist. (C) FasII IF stains γ and α/β neurons in the MB of 1-day old adult brains. In the *syp* RNAi knockdown brains there is loss of α/β neurons and excess γ neurons. There is no difference in MB morphology in the *proslong-REDr* line, compared to *wild type*.

smFISH approaches combined with genetics and biochemistry will allow the detailed disentanglement of the transcriptional and post-transcriptional mechanisms regulating these genes.

Regulating expression levels by differential mRNA isoform stability and long 3' UTRs is likely to be a conserved mechanism

Mammalian SYNCRIP/hnRNPQ is an important regulator of neural development (Lelieveld et al., 2016; Liu et al., 2015; Stoiber et al., 2015) and has a number of post-transcriptional roles including regulating mRNA stability through binding at the 3' end of transcripts (Kim et al., 2011; Kuchler et al., 2014). Prox1, the

mammalian orthologue of Pros, is a tumour suppressor that regulates stem cell differentiation in the brain as well as many other organ systems (Elsir et al., 2012; Stergiopoulos et al., 2014). Like *Drosophila pros*, *prox1* has several isoforms including alternative 3' UTRs, and a burst of Prox1 expression is required to drive the differentiation of immature granular neurons in the adult hippocampus (Hsieh, 2012). It is plausible that post-transcriptional regulation by RBPs helps determine the expression and translation of Prox1. Application of quantitative smFISH to mammalian systems will uncover whether Prox1 expression levels, like *pros*, are regulated through differential stabilisation of different 3' UTR isoforms.

MATERIALS AND METHODS

Key resources table

Reagent or resource	Source	Identifier
Antibodies		
Guinea pig anti-Syncrip (WB 1:2000, IF 1:100)	I.Davis Lab (McDermott et al. 2012)	N/A
Mouse anti-Prospero (IF 1:100)	Abcam	ab196361
Rat anti-Deadpan (IF 1:200)	Abcam	ab195173
Mouse anti- α Tubulin (WB 1:2000)	Abcam	ab7291
Rat anti-Elav	DSHB	ab528218
Licor secondary antibodies for WB (1:2500)	Licor	
Alex-Fluor secondary antibodies for IF (1:2000)	Thermo Fisher Scientific	
Bacterial strain		
Stellar™ competent cells	Takara Clontech	PT-50552
Chemicals, peptides, and recombinant proteins		
Dextran sulfate 50% solution	Sigma-Aldrich	S4030
VECTASHIELD Antifade Mounting Medium	VECTOR Laboratories	H-1000
Formaldehyde, 16%, methanol free, Ultra Pure	Polysciences, Inc.	18814-20
Critical commercial assays		
QIAPrep Spin Miniprep Kit	Qiagen	27106
Illustra™ RNAspin Mini Isolation Kit	GE Healthcare	45-001-163
Prime-a-Gene labelling system	Promega	U1100
SYBR Green qPCR Master Mix	Thermo Fisher Scientific	K0221
PCR Master Mix HotShot Diamond	Clent Life Science	HS002
LC Green Plus+	BioFire	BCHM-ASY-0005
Protein A magnetic beads	Abcam	ab214286
NEBNext® Poly(A) mRNA Magnetic Isolation Module	New England Bio Labs	E7490L
Ion Total RNA-Seq Kit v2	Thermo Fisher Scientific	4475936
Ion PI IC 200 Kit	Thermo Fisher Scientific	4488377
Taq DNA polymerase	New England Bio Labs	M0273S
TOPO® TA cloning kit for sequencing	Thermo Fisher Scientific	K4575J10
In-fusion® HD cloning kit	Takara Clontech	638906
Deposited data		
RNA sequencing data of larval brains from <i>wild type</i> and <i>syncrip</i> mutant	Gene Expression Omnibus (GEO)	GSE145670
Experimental models: organisms/strains		
<i>Drosophila: Oregon-R</i>	Bloomington	2376
<i>Drosophila: w[1118]; Df(3R)BSC124/TM6B</i>	Bloomington	9289
<i>Drosophila: PBac(PB)Syp[e00286]/TM6B</i>	Harvard Exelixis Collection	
<i>Drosophila: Df(3R)Exel7308</i>	Bloomington	7959
<i>Drosophila: Syp-RNAi</i>	Vienna <i>Drosophila</i> RNAi Center	33011, 33012
<i>Drosophila: Imp-RNAi</i>	Bloomington	34977
<i>Drosophila: vasa-Cas9</i>	Bloomington	55821
<i>Drosophila: pros-longSTOP</i>	This study	N/A
<i>Drosophila: prosΔprosUP</i>	This study	N/A
<i>Drosophila: proslong-SV40</i>	This study	N/A
<i>Drosophila: proslong-Redr</i>	This study	N/A
<i>Drosophila: insc-GAL4</i>	Betschinger et al., 2006	N/A
<i>Drosophila: OK107-GAL4</i>	Bloomington	854
<i>Drosophila: hsFLP;Pin/CyO;Tm2,Sb/Tm6b</i>	Awasaki et al., 2014	
<i>Drosophila: act>FOT>Gal4, UAS-mCD8::GFP/CyO;Tm3,Sb/Tm6b</i>	Harris et al., 2015	
Oligonucleotides		
Primers for northern blot	This study	See Table S2
Primers for RT-qPCR	This study	See Table S3
Stellaris® DNA probe set	BioResearch Technologies	See Table S4
Recombinant DNA		
pDsRed-attP	Addgene Melissa Harrison & Kate O Connor-Giles	51019
<i>P[acman]</i> BAC	BAC Resource	CH322-133M22
Software and algorithms		
Fiji ImageJ	Schindelin et al., 2012	http://imagej.nih.gov/ij
Bitplane: Imaris	<i>Bitplane</i>	http://www.bitplane.com/
Image Studio	<i>LI-COR</i>	https://www.licor.com/bio/products/software/image_studio
TopHat Aligner v2.0.13	Kim et al., 2013	https://ccb.jhu.edu/software/tophat
DeSeq 2	Bioconductor (Love et al., 2014)	https://www.licor.com/bio/products/software/image_studio
SnapGene	<i>SnapGene</i>	http://www.snapgene.com/

Contact for reagent and resource sharing

For further information and access to any reagents and fly strains used in this manuscript, please contact corresponding author Ilan Davis (ilan.davis@bioch.ox.ac.uk).

Experimental model and subject details

Fly genetics

All strains were raised on standard cornmeal-agar medium at 25°C. Oregon-R was used as the *wild type* strain.

Clonal analysis

For *wild type*, female hsFLP;Pin/CyO;Tm2,Sb/Tm6B were crossed to male act>FOT>Gal4, UAS-mCD8::GFP/CyO;Tm3,Sb/Tm6b. These lines were crossed to the *syp* mutant to produce parental lines to make the clones: female hsFLP;Pin/CyO;Syp[e00286]/Tm6b were crossed to male act>FOT>Gal4,UAS-mCD8::GFP/CyO;Syp[e00286]/Tm6b. Eggs were collected in a 4-h egg lay on apple juice plates with yeast paste at 25°C. 24 h after the egg lay, newly hatched larvae were transferred to fly food vials and incubated in a 37°C water bath for 25 min. Wandering larvae were dissected 96 h after larval hatching. For *syp* mutant, only non-tubby larvae were dissected. Immunofluorescence was completed as described below and clones were imaged on the ventral side.

pros^{long} deletion mutant generation using CRISPR

sgRNA construct design and validation was performed by Dr Andrew Bassett - Genome Engineering Oxford (GEO) (Table S5). Plasmids were injected into *vasa-cas9* embryos (Bloomington Stock: BL55821) as previously described (Bassett and Liu, 2014). For homologous recombination repair, the donor construct included a ds-RED marker for selection, flanked by lox sites to remove the dsRED, and an attP site to allow future insertions at the site. This inserted cassette was flanked by 1 kb homology arms to facilitate repair. The pDsRED-attP vector 51019 was used. Homology arms were amplified from purified BAC DNA (CH322-133M22).

Nonsense-Mediated mRNA-Decay mutant

We took advantage of the unique coding sequence that is specific to the three long isoforms of *pros*, contributing an additional 300 amino acids to the N-terminus of Pros protein. We used CRISPR/Cas9 with non-homologous end joining to induce a frame shift, which introduces a stop codon 80 bp downstream (Fig. S2A). This stop codon would be expected to produce a truncated protein and induce Nonsense mediated mRNA decay (NMD) of the *pros^{long}* transcripts. However, this line (*pros^{long}STOP*) showed no reduction in either *pros^{long}*-specific smFISH signal (Fig. S2B), or Pros protein (Fig. S2C). This result suggests that the upstream coding sequence is not actually translated in *pros^{long}* in the neurons. Instead, Pros protein is most likely produced from the downstream translation start site.

UTR extension deletion

We aimed to delete the *pros* UTR extension directly using a CRISPR strategy with homologous recombination (HR), but this was unsuccessful. We speculate that the mutant line was embryonic dominant lethal, implying unknown roles for the UTR extension or non-coding transcription from this region.

Upstream promoter deletion

We used an HR strategy to delete the three promoters that are annotated to produce the UTR extended isoform, collectively termed *pros^{long}* (Fig. S3A). We found that this line (*pros^{long}ΔpromUP*) successfully abolished transcription from the upstream promoters, but the *pros^{long}*-specific UTR probe showed substantial remaining expression, albeit reduced compared to *wild type* (Fig. S3B). Furthermore, the level of Pros protein was unchanged compared to *wild type* (Fig. S3C). We conclude that the UTR extension of *pros^{long}* can be transcribed from the downstream promoters. The lower levels of *pros^{long}* in this line are sufficient to produce the *wild type* upregulation of Pros protein in neurons.

Transcriptional termination

We designed a strategy to terminate transcription at the beginning of the 3' UTR extension using a strong SV40 transcriptional terminator. This strategy uses a two-step process to insert an attP site and then integrate the SV40 terminator. The SV40 terminator (*proslong-SV40*) did not prevent the formation of the extended UTR of *pros^{long}* (Fig. S4). Unexpectedly, the inserted *dsRED* marker used to screen for integration does terminate the UTR extension of *pros* (Fig. 6). We tested lines with the dsRED marker inserted in both orientations, which had the same phenotype. The *dsRED* inserted in the opposite orientation to *pros* (*proslong-REDr*) showed the lowest expression of dsRED allowing use of the red channel for smFISH staining, and so this line was used for further experiments.

Method details

RNA extraction

Third instar larval brains were homogenised in IP buffer (50 mM Tris-HCl pH 8.0, 150 mM NaCl, 0.5% NP-40, 10% glycerol, 1 mini tablet of Complete EDTA-free protease inhibitor and 2 µl RNase inhibitor (RNasin Plus RNase Inhibitor, Promega). RNA extraction was performed using the RNAspin Mini kit (GE Healthcare).

Western blot

NuPage Novex 4–12% Bis-Tris gels (Invitrogen) were used for all SDS-PAGE experiments. Following SDS-PAGE, proteins were transferred to nitrocellulose membrane using the XCell II™ Blot Module (Invitrogen) following the manufacturer's protocol. Protein bands were visualised with a quantitative infrared imaging system (LI-COR Odyssey).

Northern blot

5 µl of purified RNA samples was mixed with 3.5 µl 37% formaldehyde and 10 µl 100% formamide, 2 µl supplemented 10x MOPS buffer (400 mM MOPS buffer, 100 mM NaOAc, 10 mM Na₂EDTA). Sample mixture was incubated at 55°C for 15 min and 4 µl of loading dye (1 mM EDTA, 0.25% BromoPhenolBlue, 50% Glycerol) was added and run on a 1.5% agarose gel at 120 V in 1x MOPS buffer. ssRNA ladder (NEB) was used as size marker for all northern blot experiments.

RNA was transferred to pre-wet Nylon membrane (Hybond-N, Amersham). Blotted RNA was crosslinked to the membrane with either a UV crosslinker or by baking at 80°C for >1 h. The membrane was hybridised in hybridisation buffer (0.4 M Na₂HPO₄, 6% SDS and 1 mM EDTA) for 1 h at 57°C with RNA probes prepared using the Prime-a-Gene kit (Promega) (for list of primers used to generate RNA probes, see Table S2), washed twice with wash buffer 1 (40 mM Na₂HPO₄, 5% SDS and 1 mM EDTA) and twice with wash buffer 2 (40 mM Na₂HPO₄, 5% SDS and 1 mM EDTA). RNA was detected overnight in PhosphorImager (Molecular Dynamics).

Real-time quantitative PCR (RT-qPCR)

RT-qPCR was performed using a real time PCR detection system [CFX96 Touch™ Real-Time PCR Detection System (Bio-Rad)] and in 25 µl consisted of 12.5 µl 2x SYBRGreen Mastermix (Thermo Fisher Scientific), 0.75 µl of gene-specific primer (10 µM stock, forward and reverse, Table S3), 4 µl of cDNA and 7 µl of nuclease-free water. Cycle threshold value was calculated by the Bio-Rad CFX software using a second differential maximum method. For each of three biological replicates, a dilution series of the input sample was produced (10%, 2%, 0.5%, 0.01% of input). qPCR for each set of primers was performed on this series and the Cq values were plotted against log₁₀ dilution to find the formula of the line. The Cq value of each pulldown sample (anti-Syp and anti-IgG) was inputted into this formula to calculate the % of input pulled down. For each set of primers, a two-tailed Student's *t*-test was used to compare the % input pulldown in the test (anti-Syp) and control (anti-IgG) samples.

Immunoprecipitation

Guinea pig anti-Syp antibody and IgG antibody were cross linked to ProteinA magnetic beads (Abcam) following the manufacturer's protocol. For each replicate, 90 third instar larval brains dissected in Schneider's medium were homogenised in immunoprecipitation (IP) buffer (50 mM Tris-HCl pH 8.0, 150 mM NaCl, 0.5% NP-40, 10% glycerol, 1 mini tablet

of Complete EDTA-free protease inhibitor and 2 μ l RNase inhibitor [RNasin[®] Plus RNase Inhibitor (Promega)] and topped up to 100 μ l in IP buffer. For each reaction, 20 μ l of lysate was taken as a 50% input sample, which was taken directly to RNA extraction. 40 μ l of lysate was incubated with 25 μ l of each antibody cross-linked beads over night at 4°C on rotator wheel. For each reaction, 100 μ l of lysate was incubated with 20 μ l of 50% bead slurry over night at 4°C on rotator wheel. Next day, supernatant was transferred to fresh tubes and beads were washed five times for 5 min each with 200 μ l cold IP buffer at 4°C. After final wash, beads were resuspended in 40 μ l extraction buffer (50 mM Tris-HCl pH 8.0, 10 mM EDTA and 1.3% SDS, 1:100 RNasin) and incubated at 65°C, 1000 rpm for 30 min on thermomixer. The elution step was repeated and the supernatant were pooled. RNA was then extracted from the IP eluates and the input sample and used for cDNA library synthesis.

RNA sequencing

Three biological replicates ($n=3$), each replicate consists of a pool of 100 larval brains. Following RNA extraction, mRNA was enriched using NEB Next[®] Poly(A) mRNA Magnetic Isolation Module (NEB). Briefly, extracted RNA sample was mixed with Oligo d(T)₂₅ beads and heated to 65°C for 5 min followed by incubation at 4°C for 1 h to allow binding. Following incubation, the beads were washed 5 times for 5 min each at 4°C and RNA was eluted by heating the beads at 80°C for 5 min. Poly(A) enriched RNA was then used for library production using the Ion Total RNA-Seq Kit v2 for Whole Transcriptome Libraries (Life Technologies). Following quality-control steps, adaptors were hybridised to the RNA fragments and RT reaction was performed followed by cDNA amplification with Ion Xpress RNA Barcode primers. Prior to sequencing, quality of cDNA libraries were assessed using Agilent High Sensitivity DNA Kit with the Agilent 2100 Bioanalyser. Libraries were pooled to a total concentration of 100 pM, with three samples multiplexed per chip. Sequencing was performed on an Ion Proton Sequencer, using the Ion PI IC 200 Kit (Life Technologies). Ion PI chips were prepared following the manufacturer's instructions and loaded using the Ion Chef System.

Immunofluorescence

Third instar larval brains were dissected in Schneider's medium and fixed in 4% formaldehyde solution (4% formaldehyde in 0.3% PBTX), for 25 min at room temperature. Following incubation with primary and secondary antibody, samples were mounted in VECTASHIELD anti-fade mounting medium (Vector Laboratories). All imaging experiments were performed with three replicates and representative images are shown.

RNA smFISH for larval brains

Dissected third instar larval brains were fixed in 4% paraformaldehyde solution for 25 min at room temperature followed by three rinses in 0.3% PBTX (PBS and 0.3% triton-X). Samples were washed three times for 15 min each in 0.3% PBTX at room temperature and incubated in pre-hybridisation buffer (10% deionised formamide in prepared in 2 \times SSC) for 5 min at 37°C. Hybridisation was performed by incubating samples overnight at 37°C in the dark with gentle shaking in hybridisation buffer [10% deionised formamide, 5% dextran sulphate (Sigma-Aldrich), 2 \times SSC] containing 250 nM gene-specific fluorescently labelled Stellaris[®] DNA probe set (BioSearch Technologies). Following hybridisation, samples were rinsed three times in pre-hybridisation buffer and washed a further three times, for 15 min each time in pre-hybridisation buffer at 37°C. DAPI was included during the second 15 min wash. Samples were mounted in VECTASHIELD anti-fade mounting medium (Vector Laboratories) and imaged. Samples were protected from light for all steps including hybridisation.

smFISH with immunofluorescence for larval brains

For smFISH with anti-Dpn antibody, the smFISH was performed identically as above, then, after washing three times 30 min in pre-hybridisation buffer on Day 2, samples were blocked in blocking buffer (1% BSA in 0.3% PBTX) for 1 h at room temperature. Samples were incubated with primary antibody in blocking buffer for 3 h at room temperature, washed, and then incubated with secondary antibody for 1 h at room temperature. Final washes were performed using 0.3% PBTX, once including DAPI.

For all other antibodies, the protocol is identical to the smFISH protocol with the following modifications. Before hybridisation, samples were blocked in blocking buffer (1% BSA in 0.3% PBTX) for 1 h at room temperature. Antibody at the appropriate dilution was included with the Stellaris[®] DNA probes during the overnight hybridisation step. Counterstain with secondary antibody was performed on the second day following hybridisation. After final wash, samples were mounted in VECTASHIELD anti-fade mounting medium (Vector Laboratories) and immediately imaged.

Image acquisition

Larval brains were imaged on the ventral side. Fixed imaging of larval brains was performed using an inverted Olympus FV3000 Laser Scanning Microscope with Becker and Hickel FLIM system and with an inverted Olympus FV1200 Laser Scanning Microscope with high sensitivity gallium arsenide phosphide (GaAsP) detectors (Olympus). Images were acquired using $\times 20$ 0.75 NA UPlanSApo, $\times 40$ 1.3 NA Oil UPlan FLN, $\times 60$ 1.4 NA and $\times 100$ 1.4 NA Oil UPlanSApo objective lenses. The laser units used were solid state 405 and 488 lasers, argon 488, 515, 568 and 633 lasers.

Quantification and statistical analysis

Bioinformatic analysis of RNA sequencing data

Base calling, read trimming and sample de-multiplexing were done using the standard Ion Torrent Suite. The reads were aligned to the *Drosophila* genome (ENSEMBL assembly BDGP5, downloaded 8 Jan 2015) using the TopHat aligner (v2.0.13) (Kim et al., 2013). To quantitate gene expression, uniquely aligned reads were assigned to the *Drosophila* exome (BDGP5) using htseq-count. Differential was assessed using negative binomial generalised linear models implemented in R/Bioconductor package DESeq2 (Love et al., 2014). Differential expression analysis is presented in Table S1.

Image analysis for smFISH

pros intron probes were used to compare *pros* transcription rates in *wild type* and *syp* mutant brains (Fig. 3E). Transcription rates were compared separately for type I NBs and for progeny cells (including GMCs, immature and mature neurons). *pros* intron transcription foci were identified in 3D with the spot detection feature of Imaris Image Analysis software (*Imaris, Bitplane*), using a 1.2 μ m diameter spot. Spots overlapping the edge of the image were removed. Average intensity was measured for each spot.

In type I NBs, *pros* transcription foci are found spatially separated in the nucleus and therefore the intensity of two spots were added together for each NB. In progeny cells, the transcription foci are close in the nucleus and are measured in a single spot. Intensity measurements were normalised to the average *wild type* intensity for each experimental replicated (i.e. the average of *wild type* measurements from a single day of staining/imaging).

Acknowledgements

We are grateful to Andrew Bassett (Genome Engineering Oxford, GEO) for assistance in designing and validating CrispR guide RNAs, to Tomek Dobrzycki for initial work that lead to the project, to MICRON Oxford (<http://micronoxford.com>), supported by a Wellcome Strategic Awards to I.D. (091911/B/10/Z and 107457/Z/15/Z) providing access to equipment and advice on advanced imaging techniques, to Alan Wainman and Richard M. Parton for advice on advanced microscopy and to Darragh Ennis for help and advice with fly husbandry and administration. We are also indebted to Alfredo Castello, Lidia Vasilieva, Jordan Raff and Neil Brockdorff for their comments. We would also like to thank the Cambridge Fly Facility for transgenic production and the Bloomington *Drosophila* Stock Centre.

Competing interests

The authors declare no competing or financial interests.

Author contributions

Conceptualization: T.J.S., L.Y., D.I.-H., I.D.; Methodology: T.J.S., Y.A., A.I.J., F.R., J.Y.L., L.Y., C.-P.Y., T.L., D.I.-H., I.D.; Software: A.I.J.; Formal analysis: T.J.S., Y.A., J.Y.L.; Investigation: T.J.S., Y.A., J.Y.L.; Writing - original draft: T.J.S., L.Y.; Writing - review & editing: T.J.S., D.I.-H., I.D.; Visualization: T.J.S., A.I.J.; Supervision: I.D.; Funding acquisition: I.D., T.L.

Funding

T.J.S. was funded by Wellcome Trust Four-Year PhD Studentship (105363/Z/14/Z). L.Y. was funded from the Clarendon Trust and Goodger Fund. F.R. was funded by a

Marie Curie Postdoctoral Fellowship. C.-P.Y. and T.L. were supported by Howard Hughes Medical Institute. J.Y.L. was funded by the Clarendon Trust. D.I.-H. was funded by University College London. A.I.J. was funded by a Wellcome Senior Research Fellowship to I. D. (096144Z/17/Z). F. R. was funded by a Wellcome Investigator Award to I.D. (209412Z/17/Z).

Data availability

The presented RNA sequencing data has been deposited with Gene Expression Omnibus (GEO), with accession number GSE145670.

Supplementary information

Supplementary information available online at <http://bio.biologists.org/lookup/doi/10.1242/bio.049684.supplemental>

References

- Awasaki, T., Kao, C., Lee, Y., Yang, C., Huang, Y., Pfeiffer, B. D., Luan, H., Jing, X., Huang, Y., He, Y. et al. (2014). Making *Drosophila* lineage-restricted drivers via patterned recombination in neuroblasts. *Nature Neuroscience*, **17**, 631-7
- Bassett, A. and Liu, J.-L. (2014). CRISPR/Cas9 mediated genome engineering in *Drosophila*. *Methods* **69**, 128-136. doi:10.1016/j.ymeth.2014.02.019
- Bayraktar, O. A., Boone, J. Q., Drummond, M. L. and Doe, C. Q. (2010). *Drosophila* type II neuroblast lineages keep Prospero levels low to generate large clones that contribute to the adult brain central complex. *Neural Dev.* **5**, 26. doi:10.1186/1749-8104-5-26
- Bello, B., Reichert, H. and Hirth, F. (2006). The brain tumor gene negatively regulates neural progenitor cell proliferation in the larval central brain of *Drosophila*. *Development* **133**, 2639-2648. doi:10.1242/dev.02429
- Berger, C., Harzer, H., Burkard, T. R., Steinmann, J., van der Horst, S., Laurenson, A.-S., Novatchkova, M., Reichert, H. and Knoblich, J. A. (2012). FACS purification and transcriptome analysis of *Drosophila* neural stem cells reveals a role for Klumpfuss in self-renewal. *Cell Rep.* **2**, 407-418. doi:10.1016/j.celrep.2012.07.008
- Betschinger, J., Mechtler, K. and Knoblich, J. A. (2006). Asymmetric segregation of the tumor suppressor *brat* regulates self-renewal in *Drosophila* neural stem cells. *Cell* **124**, 1241-1253. doi:10.1016/j.cell.2006.01.038
- Carney, T. D., Struck, A. J. and Doe, C. Q. (2013). *midlife* encodes a conserved zinc-finger protein required to maintain neuronal differentiation in *Drosophila*. *Development* **140**, 4155-4164. doi:10.1242/dev.093781
- Choksi, S. P., Southall, T. D., Bossing, T., Edoff, K., de Wit, E., Fischer, B. E., van Steensel, B., Micklem, G. and Brand, A. H. (2006). Prospero acts as a binary switch between self-renewal and differentiation in *Drosophila* neural stem cells. *Dev. Cell* **11**, 775-789. doi:10.1016/j.devcel.2006.09.015
- Davie, K., Janssens, J., Koldere, D., De Waegeneer, M., Pech, U., Kreft, L., Aibar, S., Makhzami, S., Christiaens, V., Bravo González-Blas, C. et al. (2018). A single-cell transcriptome atlas of the aging *Drosophila* brain. *Cell* **174**, 982-998.e920. doi:10.1016/j.cell.2018.05.057
- Doe, C. Q., Chu-LaGra, Q., Wright, D. M. and Scott, M. P. (1991). The prospero gene specifies cell fates in the *Drosophila* central nervous system. *Cell* **65**, 451-464. doi:10.1016/0092-8674(91)90463-9
- Elsir, T., Smits, A., Lindström, M. S. and Nistér, M. (2012). Transcription factor PROX1: its role in development and cancer. *Cancer Metastasis Rev.* **31**, 793-805. doi:10.1007/s10555-012-9390-8
- Grosskortenhaus, R., Robinson, K. J. and Doe, C. Q. (2006). Pdm and Castor specify late-born motor neuron identity in the NB7-1 lineage. *Genes Dev.* **20**, 2618-2627. doi:10.1101/gad.1445306
- Harris, R. M., Pfeiffer, B. D., Rubin, G. M. and Truman, J. W., (2015). Neuron hemilineages provide the functional ground plan for the *Drosophila* ventral nervous system. *eLife*. **20**
- Hilgers, V. (2015). Alternative polyadenylation coupled to transcription initiation: Insights from ELAV-mediated 3' UTR extension. *RNA Biol.* **12**, 918-921. doi:10.1080/15476286.2015.1060393
- Hilgers, V., Perry, M. W., Hendrix, D., Stark, A., Levine, M. and Haley, B. (2011). Neural-specific elongation of 3' UTRs during *Drosophila* development. *Proc. Natl. Acad. Sci. USA* **108**, 15864-15869. doi:10.1073/pnas.1112672108
- Hilgers, V., Lemke, S. B. and Levine, M. (2012). ELAV mediates 3' UTR extension in the *Drosophila* nervous system. *Genes Dev.* **26**, 2259-2264. doi:10.1101/gad.199653.112
- Hirata, J., Nakagoshi, H., Nabeshima, Y. and Matsuzaki, F. (1995). Asymmetric segregation of the homeodomain protein Prospero during *Drosophila* development. *Nature* **377**, 627-630. doi:10.1038/377627a0
- Homem, C. C. F. and Knoblich, J. A. (2012). *Drosophila* neuroblasts: a model for stem cell biology. *Development* **139**, 4297-4310. doi:10.1242/dev.080515
- Hsieh, J. (2012). Orchestrating transcriptional control of adult neurogenesis. *Genes Dev.* **26**, 1010-1021. doi:10.1101/gad.187336.112
- Isshiki, T., Pearson, B., Holbrook, S. and Doe, C. Q. (2001). *Drosophila* neuroblasts sequentially express transcription factors which specify the temporal identity of their neuronal progeny. *Cell* **106**, 511-521. doi:10.1016/S0092-8674(01)00465-2
- Kambadur, R., Koizumi, K., Stivers, C., Nagle, J., Poole, S. J. and Odenwald, W. F. (1998). Regulation of POU genes by castor and hunchback establishes layered compartments in the *Drosophila* CNS. *Genes Dev.* **12**, 246-260. doi:10.1101/gad.12.2.246
- Kelava, I. and Lancaster, M. A. (2016). Stem cell models of human brain development. *Cell Stem Cell* **18**, 736-748. doi:10.1016/j.stem.2016.05.022
- Kim, D.-Y., Kwak, E., Kim, S.-H., Lee, K.-H., Woo, K.-C. and Kim, K.-T. (2011). hnRNP Q mediates a phase-dependent translation-coupled mRNA decay of mouse Period3. *Nucleic Acids Res.* **39**, 8901-8914. doi:10.1093/nar/gkr605
- Kim, D., Perte, G., Trapnell, C., Pimentel, H., Kelley, R. and Salzberg, S. L. (2013). TopHat2: accurate alignment of transcriptomes in the presence of insertions, deletions and gene fusions. *Genome Biol.* **14**, R36. doi:10.1186/gb-2013-14-4-r36
- Kitajima, A., Fuse, N., Isshiki, T. and Matsuzaki, F. (2010). Progenitor properties of symmetrically dividing *Drosophila* neuroblasts during embryonic and larval development. *Dev. Biol.* **347**, 9-23. doi:10.1016/j.ydbio.2010.06.029
- Knoblich, J. A. (2008). Mechanisms of asymmetric stem cell division. *Cell* **132**, 583-597. doi:10.1016/j.cell.2008.02.007
- Knoblich, J. A., Jan, L. Y. and Jan, Y. N. (1995). Asymmetric segregation of *numb* and *prospero* during cell division. *Nature* **377**, 624-627. doi:10.1038/377624a0
- Kohwi, M. and Doe, C. Q. (2013). Temporal fate specification and neural progenitor competence during development. *Nat. Rev. Neurosci.* **14**, 823-838. doi:10.1038/nrn3618
- Kuchler, L., Giegerich, A. K., Sha, L. K., Knape, T., Wong, M. S., Schröder, K., Brandes, R. P., Heide, H., Wittig, I., Brune, B. et al. (2014). SYNCRIP-dependent Nox2 mRNA destabilization impairs ROS formation in M2-polarized macrophages. *Antioxid Redox Signal.* **21**, 2483-2497. doi:10.1089/ars.2013.5760
- Lai, S. L. and Doe, C. Q. (2014). Transient nuclear Prospero induces neural progenitor quiescence. *Elife* **3**, e03363. doi:10.7554/eLife.03363.013
- Lee, C.-Y., Wilkinson, B. D., Siegrist, S. E., Wharton, R. P. and Doe, C. Q. (2006). *Brat* is a Miranda cargo protein that promotes neuronal differentiation and inhibits neuroblast self-renewal. *Dev. Cell* **10**, 441-449. doi:10.1016/j.devcel.2006.01.017
- Lelieveld, S. H., Reijnders, M. R. F., Pfundt, R., Yntema, H. G., Kamsteeg, E.-J., de Vries, P., de Vries, B. B. A., Willemsen, M. H., Kleefstra, T., Lohner, K. et al. (2016). Meta-analysis of 2,104 trios provides support for 10 new genes for intellectual disability. *Nat. Neurosci.* **19**, 1194-1196. doi:10.1038/nn.4352
- Li, X., Erclik, T., Bertet, C., Chen, Z., Voutev, R., Venkatesh, S., Morante, J., Celik, A. and Desplan, C. (2013). Temporal patterning of *Drosophila* medulla neuroblasts controls neural fates. *Nature* **498**, 456-462. doi:10.1038/nature12319
- Liu, Z., Yang, C.-P., Liu, S., Sugino, K., Fu, C.-C., Liu, L.-Y., Yao, X., Lee, L. P. and Lee, T. (2015). Opposing intrinsic temporal gradients guide neural stem cell production of varied neuronal fates. *Science* **350**, 317-320. doi:10.1126/science.1251886
- Love, M. I., Huber, W. and Anders, S. (2014). Moderated estimation of fold change and dispersion for RNA-seq data with DESeq2. *Genome Biol.* **15**, 550. doi:10.1186/s13059-014-0550-8
- Matsuzaki, F., Koizumi, K., Hama, C., Yoshioka, T. and Nabeshima, Y. (1992). Cloning of the *Drosophila prospero* gene and its expression in ganglion mother cells. *Biochem. Biophys. Res. Commun.* **182**, 1326-1332. doi:10.1016/0006-291X(92)91878-T
- Maurange, C., Cheng, L. and Gould, A. P. (2008). Temporal transcription factors and their targets schedule the end of neural proliferation in *Drosophila*. *Cell* **133**, 891-902. doi:10.1016/j.cell.2008.03.034
- McDermott, S. M., Meignin, C., Rappsilber, J. and Davis, I. (2012). *Drosophila* syncrip binds the gurken mRNA localisation signal and regulates localised transcripts during Axis specification. *Biology Open* **1**, 488-497. doi:10.1242/bio.2012885
- McDermott, S. M., Yang, L., Halstead, J. M., Hamilton, R. S., Meignin, C. and Davis, I. (2014). *Drosophila* Syncrip modulates the expression of mRNAs encoding key synaptic proteins required for morphology at the neuromuscular junction. *RNA* **20**, 1593-1606. doi:10.1261/rna.045849.114
- Narbonne-Reveau, K., Lanet, E., Dillard, C., Foppolo, S., Chen, C. H., Parrinello, H., Rialle, S., Sokol, N. S. and Maurange, C. (2016). Neural stem cell-encoded temporal patterning delineates an early window of malignant susceptibility in *Drosophila*. *Elife* **5**, e13463. doi:10.7554/eLife.13463.040
- Novotny, T., Eiselt, R. and Urban, J. (2002). Hunchback is required for the specification of the early sublineage of neuroblast 7-3 in the *Drosophila* central nervous system. *Development* **129**, 1027-1036.
- Oktaba, K., Zhang, W., Lotz, T. S., Jun, D. J., Lemke, S. B., Ng, S. P., Esposito, E., Levine, M. and Hilgers, V. (2015). ELAV links paused Pol II to alternative polyadenylation in the *Drosophila* nervous system. *Mol. Cell* **57**, 341-348. doi:10.1016/j.molcel.2014.11.024
- Pearson, B. J. and Doe, C. Q. (2003). Regulation of neuroblast competence in *Drosophila*. *Nature* **425**, 624-628. doi:10.1038/nature01910
- Ren, Q., Yang, C.-P., Liu, Z., Sugino, K., Mok, K., He, Y., Ito, M., Nern, A., Otsuna, H. and Lee, T. (2017). Stem cell-intrinsic, seven-up-triggered temporal factor gradients diversify intermediate neural progenitors. *Curr. Biol.* **27**, 1303-1313. doi:10.1016/j.cub.2017.03.047
- Samuels, T. J., Järvelin, A. I., Ish-Horowicz, D. and Davis, I. (2020). Imp/IGF2BP levels modulate individual neural stem cell growth and division through myc mRNA stability. *eLife Sci.* **9**, e51529. doi:10.7554/eLife.51529

- Schindelin, J., Arganda-Carreras, I., Frise, E., Kaynig, V., Longair, M., Pietzsch, T., Preibisch, S., Rueden, C., Saalfeld, S., Schmid, B. et al.** (2012). Fiji: an open-source platform for biological-image analysis. *Nat Methods*. doi:10.1038/nmeth.2019
- Siegrist, S. E., Haque, N. S., Chen, C.-H., Hay, B. A. and Hariharan, I. K.** (2010). Inactivation of both Foxo and reaper promotes long-term adult neurogenesis in *Drosophila*. *Curr. Biol.* **20**, 643-648. doi:10.1016/j.cub.2010.01.060
- Spana, E. P. and Doe, C. Q.** (1995). The prospero transcription factor is asymmetrically localized to the cell cortex during neuroblast mitosis in *Drosophila*. *Development* **121**, 3187-3195.
- Srinivasan, S., Peng, C. Y., Nair, S., Skeath, J. B., Spana, E. P. and Doe, C. Q.** (1992). Biochemical analysis of prospero protein during asymmetric cell division: cortical prospero is highly phosphorylated relative to nuclear prospero. *Dev. Biol.* **204**. doi:10.1006/dbio.1998.9079
- Stergiopoulos, A., Elkouris, M. and Politis, P. K.** (2014). Prospero-related homeobox 1 (Prox1) at the crossroads of diverse pathways during adult neural fate specification. *Front. Cell Neurosci.* **8**, 454. doi:10.3389/fncel.2014.00454
- Stoiber, M. H., Olson, S., May, G. E., Du, M. O., Manent, J., Obar, R., Guruharsha, K. G., Bickel, P. J., Artavanis-Tsakonas, S., Brown, J. B. et al.** (2015). Extensive cross-regulation of post-transcriptional regulatory networks in *Drosophila*. *Genome Res.* **25**, 1692-1702. doi:10.1101/gr.182675.114
- Syed, M. H., Mark, B. and Doe, C. Q.** (2017). Steroid hormone induction of temporal gene expression in *Drosophila* brain neuroblasts generates neuronal and glial diversity. *Elife* **6**, e26287. doi:10.7554/eLife.26287.021
- Tekotte, H., Berdnik, D., Torok, T., Buszczak, M., Jones, L. M., Cooley, L., Knoblich, J. A. and Davis, I.** (2002). Dcas is required for importin- α 3 nuclear export and mechano-sensory organ cell fate specification in *Drosophila*. *Dev. Biol.* **244**, 396-406. doi:10.1006/dbio.2002.0612
- Thurmond, J., Goodman, J. L., Strelets, V. B., Attrill, H., Gramates, L. S., Marygold, S. J., Matthews, B. B., Millburn, G., Antonazzo, G., Trovisco, V. et al.** (2019). FlyBase 2.0: the next generation. *Nucleic Acids Res.* **47**, D759-D765.
- Vaessin, H., Grell, E., Wol, E., Bier, E., Jan, L. Y. and Jan, Y. N.** (1991). prospero is expressed in neuronal precursors and encodes a nuclear protein that is involved in the control of axonal outgrowth in *Drosophila*. *Cell* **67**, 941-953. doi:10.1016/0092-8674(91)90367-8
- Yang, C.-P., Samuels, T. J., Huang, Y., Yang, L., Ish-Horowicz, D., Davis, I. and Lee, T.** (2017a). Imp and Syp RNA-binding proteins govern decommissioning of *Drosophila* neural stem cells. *Development* **144**, 3454-3464. doi:10.1242/dev.149500
- Yang, L., Titlow, J., Ennis, D., Smith, C., Mitchell, J., Young, F. L., Waddell, S., Ish-Horowicz, D. and Davis, I.** (2017b). Single molecule fluorescence in situ hybridisation for quantitating post-transcriptional regulation in *Drosophila* brains. *Methods* **126**, 166-176. doi:10.1016/j.ymeth.2017.06.025